Magnetism with density functional theory

Spin density functional theory

Bluegel, IFF Spring School ('14)

Kohn-Sham formulation of DFT

$$[-\frac{\hbar^2}{2m}\nabla^2 + v(\mathbf{r}) + \int \frac{n(\mathbf{r}')}{|\mathbf{r}-\mathbf{r}'|}d\mathbf{r}' + \frac{\delta E_{XC}}{\delta n(\mathbf{r})}]\phi_i(\mathbf{r}) = \epsilon_i\phi_i(\mathbf{r})$$

$$n(\mathbf{r}) = \sum_{i=1}^{N} |\phi_i(\mathbf{r})|^2$$

Generalization to spin DFT (Barth & Hedin (1972))

2x2 spin-density matrix

$$n_{\alpha\beta}(\mathbf{r}) = \sum_{i=1}^{N} \phi_i^{*\alpha}(\mathbf{r})\phi_i^{\beta}(\mathbf{r})$$

$$\underline{\mathrm{n}}(\mathbf{r}) = \frac{1}{2}(n(\mathbf{r})\mathrm{I} + \sigma \cdot \mathbf{m}(\mathbf{r}))$$

$$= \frac{1}{2}\begin{pmatrix} n(\mathbf{r}) + m_z(\mathbf{r}) & m_x(\mathbf{r}) - im_y(\mathbf{r}) \\ m_x(\mathbf{r}) + im_y(\mathbf{r}) & n(\mathbf{r}) - m_z(\mathbf{r}) \end{pmatrix}$$

Spin density functional theory (contd.)

Similarly, potential matrices are written as

$$\underline{\mathrm{v}}(\mathbf{r}) = v(\mathbf{r})\mathrm{I} + \mu_B \sigma \cdot \mathbf{B}(\mathbf{r})$$

$$\underline{\mathrm{v}}_{\mathrm{XC}}(\mathbf{r}) = v_{\mathrm{XC}}(\mathbf{r})\mathrm{I} + \mu_B \sigma \cdot \mathbf{B}_{\mathrm{XC}}(\mathbf{r})$$

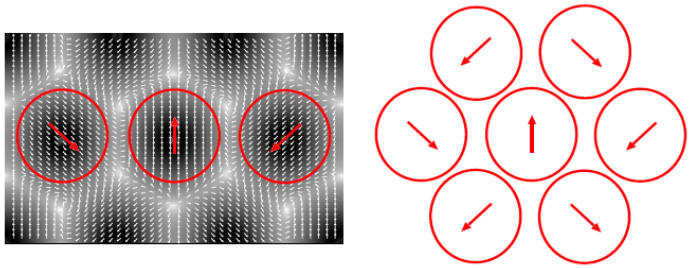

Magnetic ground state of hexagonal Cr monolayer

For collinear case

$$(\frac{\hbar^2}{2m}\nabla^2 + v_{Coul}(\mathbf{r}) + B_z(\mathbf{r}) + v^{\uparrow}_{XC}(\mathbf{r}))\phi^{\uparrow}_i(\mathbf{r}) = \epsilon^{\uparrow}_i \phi^{\uparrow}_i(\mathbf{r})$$

$$(\frac{\hbar^2}{2m}\nabla^2 + v_{Coul}(\mathbf{r}) - B_z(\mathbf{r}) + v^{\downarrow}_{XC}(\mathbf{r}))\phi^{\downarrow}_i(\mathbf{r}) = \epsilon^{\downarrow}_i \phi^{\downarrow}_i(\mathbf{r})$$

Performance of DFT

Comparison between theory and experiment

Property	source	Fe (bcc)	Co (fcc)	Ni (fcc)	Gd (hcp)
M_{spin}	LSDA	2.15	1.56	0.59	7.63
M_{spin}	GGA	2.22	1.62	0.62	7.65
M_{spin}	experiment	2.12	1.57	0.55	
$M_{tot.}$	experiment	2.22	1.71	0.61	7.63

Random binary alloys

Slater-Pauling curve

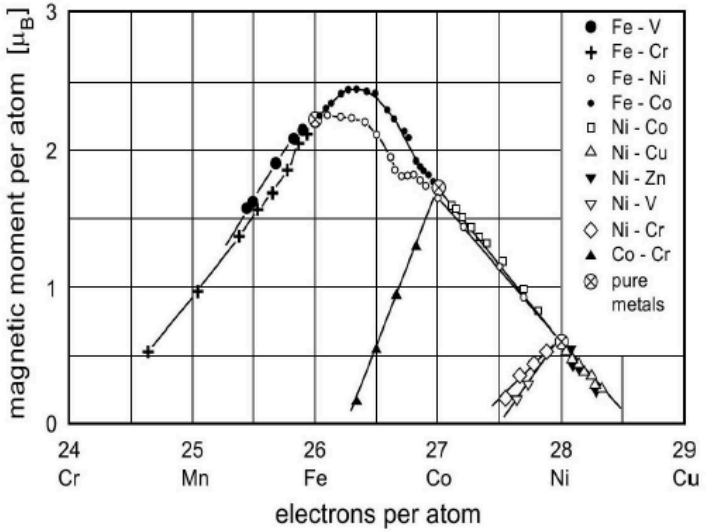

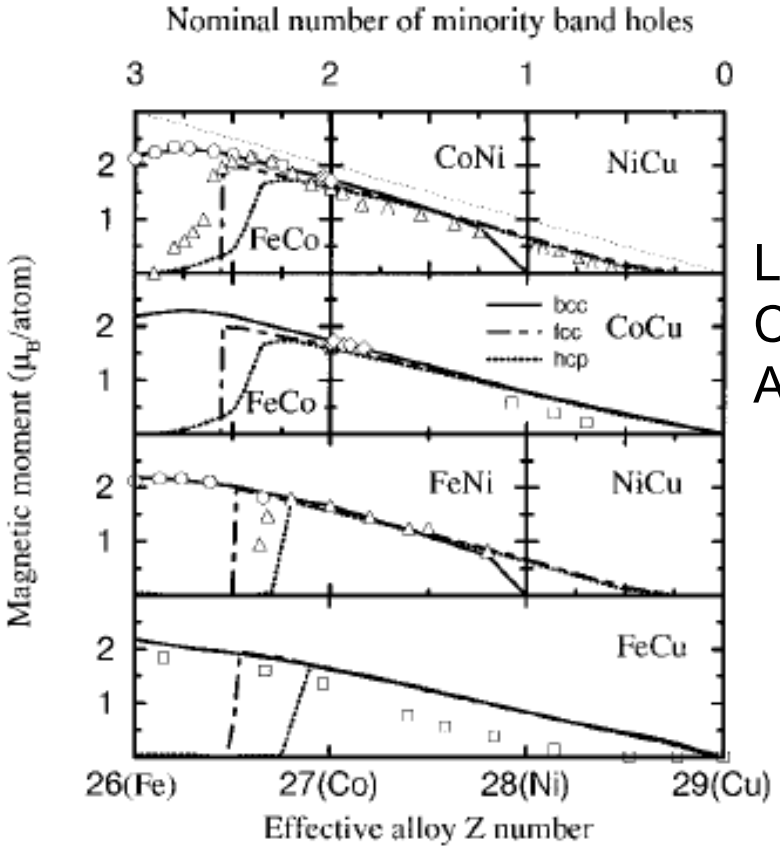

LMTO + Coherent Potential Approximation (CPA)

PRB **59**, 419 (1999)

Element-specific magnetic measurements

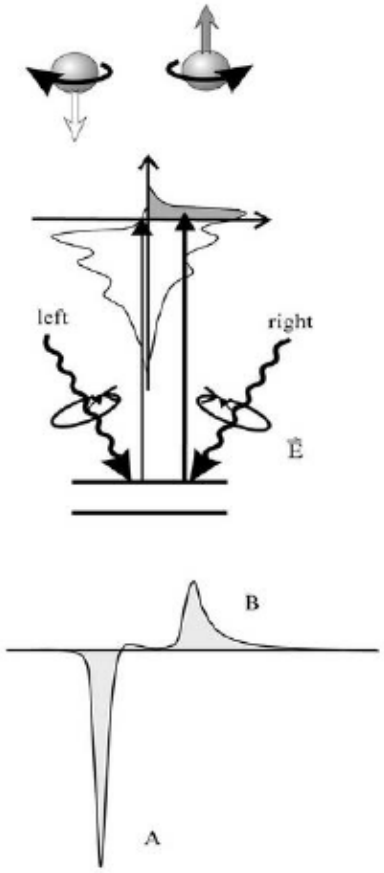

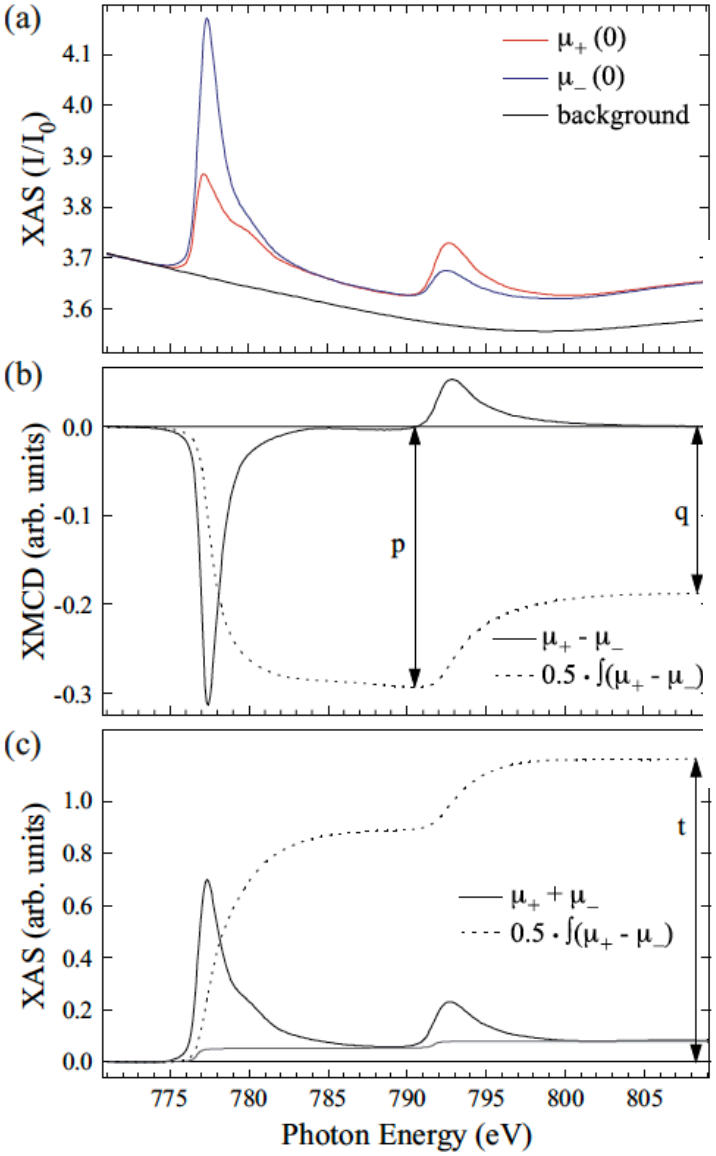

Sum rules

spin and orbital moments

$$L = -\frac{4}{3}h_d \frac{\int_{L_3+L_2}(\mu_+ - \mu_-)dE}{\int_{L_3+L_2}(\mu_+ + \mu_-)dE} = -\frac{4}{3}h_d\frac{q}{t}, \quad (1)$$

$$S + 7D = -h_d \frac{6\int_{L_3}(\mu_+ - \mu_-)dE - 4\int_{L_3+L_2}(\mu_+ - \mu_-)dE}{\int_{L_3+L_2}(\mu_+ + \mu_-)dE}$$

$$= -h_d\frac{6p - 4q}{t}, \quad (2)$$

XAS: X-ray absorption spectroscopy

XMCD: X-ray magnetic circular dichroism

Spin-dipolar contribution

Spin dipole operator:

$$T = \sum_i \left[s^{(i)} - 3\frac{r^{(i)}(r^{(i)} \cdot s^{(i)})}{\left|r^{(i)}\right|^2} \right]$$

XMCD: $m_{eff}=m_S+7\langle T_z\rangle$

Angular dependence

$$m_{eff}(\theta) = m_S + 7T(\theta)$$
$$T(\theta) \sim \frac{1}{2}(3Cos^2\theta - 1)$$

PRB **82**, 014405 (2010)

$$T = \sum_i Q^{(i)} s^{(i)}$$

Quadrupolar tensor $Q^{(i)}_{\alpha\beta} = \delta_{\alpha\beta} - 3\hat{r}^{(i)}_{\alpha}\hat{r}^{(i)}_{\beta}$

$$T_{\pm} = \sum_{\nu\nu'} T^{(\pm)}_{\nu\nu'} a^{+}_{\nu} a_{\nu'} \qquad T_z = \sum_{\nu\nu'} T^{(z)}_{\nu\nu'} a^{+}_{\nu} a_{\nu'} \qquad c^{(l)}_m(\hat{r}) = \sqrt{\frac{4\pi}{2l+1}} Y_{lm}(\hat{r})$$

$$T^{(\pm)}_{\nu\nu'} = \left\langle \nu \left| c^{(2)}_0 s_{\pm} - \sqrt{6} c^{(2)}_{\pm 2} s_{\mp} \pm \sqrt{6} c^{(2)}_{\pm 1} s_z \right| \nu' \right\rangle \qquad |\nu\rangle = |l, m, \sigma\rangle$$

$$T^{(z)}_{\nu\nu'} = \left\langle \nu \left| -\sqrt{\frac{3}{2}} c^{(2)}_{-1} s_{+} + \sqrt{\frac{3}{2}} c^{(2)}_{1} s_{-} - 2c^{(2)}_0 s_z \right| \nu' \right\rangle$$

Crystal field

No spin-flip

Oguchi and Shishidou, Phys. Rev. B **70**, 024412 (2004).

Importance of spin-dipolar contribution

Verwey transition (cubic -> monoclinic)

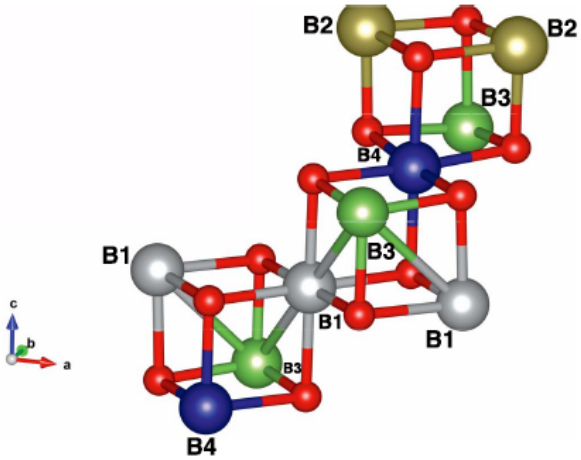

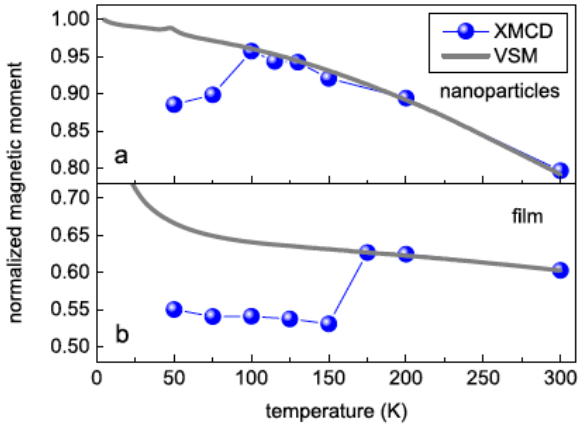

Table I | Charge, spin and magnetic dipole moments for 3d orbitals of Fe atoms at different sites in the monoclinic unit cell. Also, effective moments ($\mu_{S,eff} = -2\langle S_z\rangle \mu_B + 7\langle T_z\rangle \mu_B$) are provided. The Fe sites are named as in Ref. [17]

Fe site	d-charge	$-2\langle S_z\rangle$	$7\langle T_z\rangle$	$\mu_{S,eff}$ (μ_B)
A1	5.91	−3.98	−0.015	−3.995
A2	5.91	−3.98	0.025	−3.955
B1	6.08	3.67	0.72	4.39
B2	5.82	4.14	0.043	4.183
B3	5.85	4.08	0.027	4.107
B4	6.1	3.64	−1.44	2.20

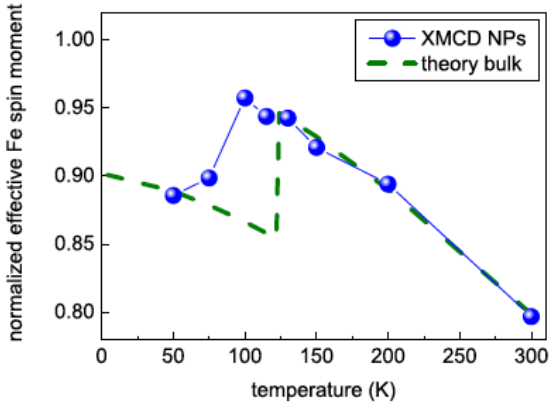

Sci. Rep. **4**, 5760 (2014)

Finite temperature magnetism
(DFT + Monte Carlo simulations)

Step 1

Map DFT to an effective spin model

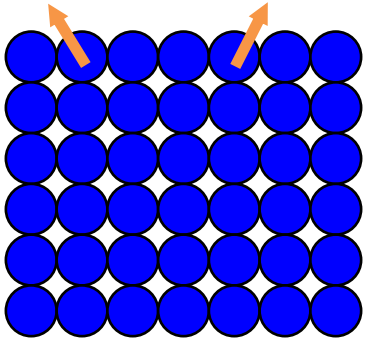

Classical Heisenberg Hamiltonian

$$H = -\sum_{i \neq j} J_{ij} \vec{e}_i \vec{e}_j$$

$$J_{ij} = \frac{1}{4\pi} \int^{E_F} dE \, \mathrm{Im}\{Tr_L(\Delta_i T_{\uparrow}^{ij} \Delta_j T_{\downarrow}^{ji})\}$$

$$\Delta_i = t_{i\uparrow}^{-1} - t_{i\downarrow}^{-1}$$

T : scattering path operator

t : on-site scattering matrix

J_{ij}>0, ferromagnetic

J_{ij}<0, antiferromagnetic

Finite temperature magnetism (contd.)

Step 2 Monte-Carlo simulations

$$H = -\sum_{i \neq j} J_{ij} \vec{e}_i . \vec{e}_j$$

Metropolis algorithm

Determination of critical temperature :

4^{th} order cumulant crossing method

$$U_L = 1 - \frac{< M^4 >}{3 < M^2 >^2}$$

M : magnetization (order parameter)

Also from magnetization/susceptibility/specific heat vs. temperature

Finite temperature magnetism (contd.)

Interatomic exchange parameters

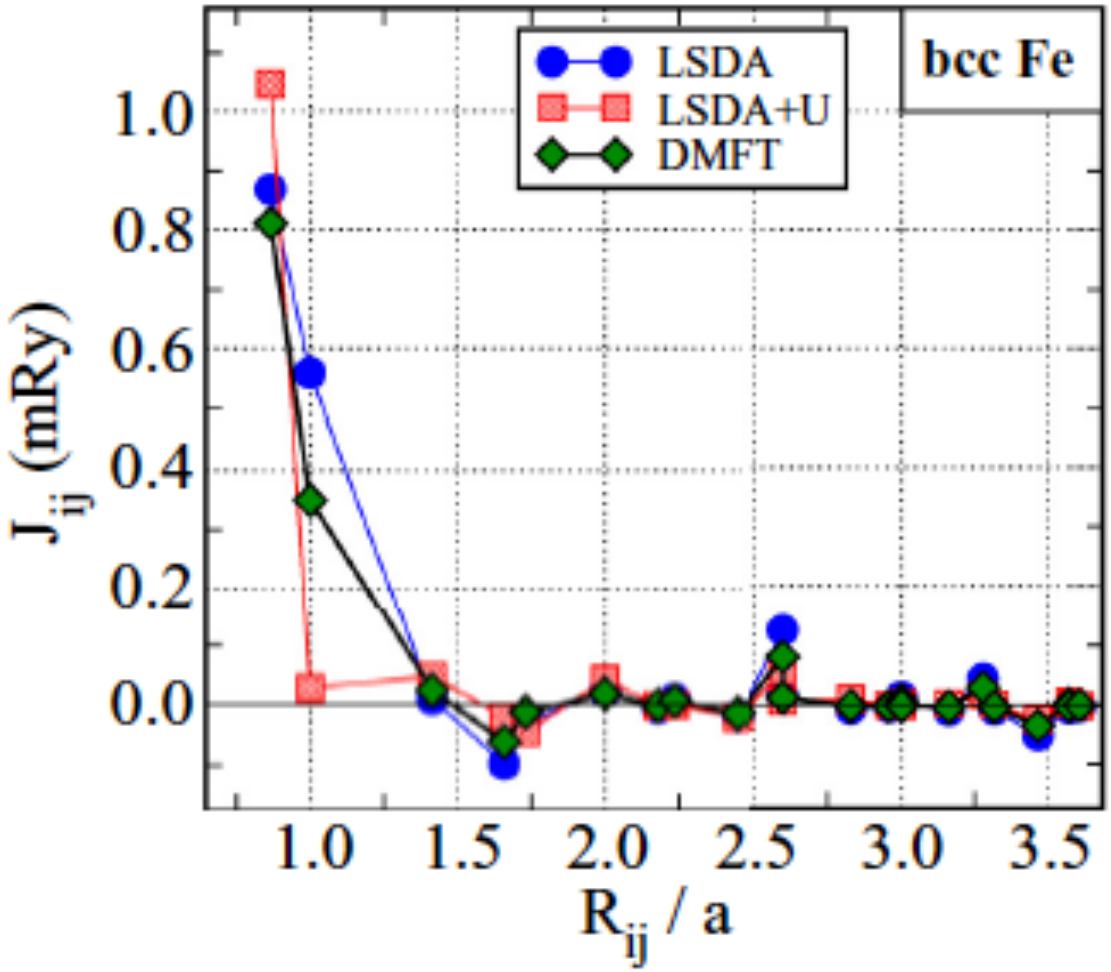

Kvashnin et al., PRB **91**, 125133 (2015)

Orbital-decomposed exchange parameters

$$J_{ij} = J_{ij}^{E_g - E_g} + J_{ij}^{E_g - T_{2g}} + J_{ij}^{T_{2g} - T_{2g}}$$

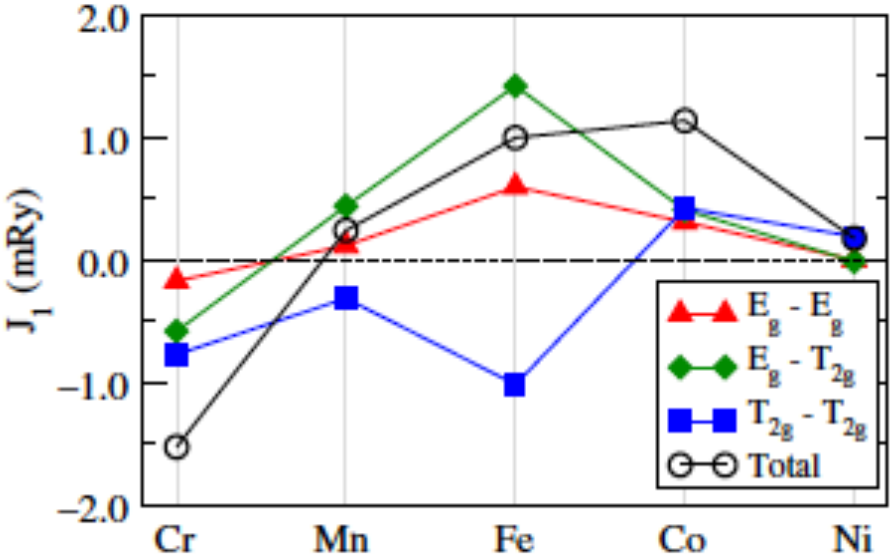

Fe and Mn are different from others

T_{2g}-T_{2g} and E_g-E_g interactions are opposite in sign

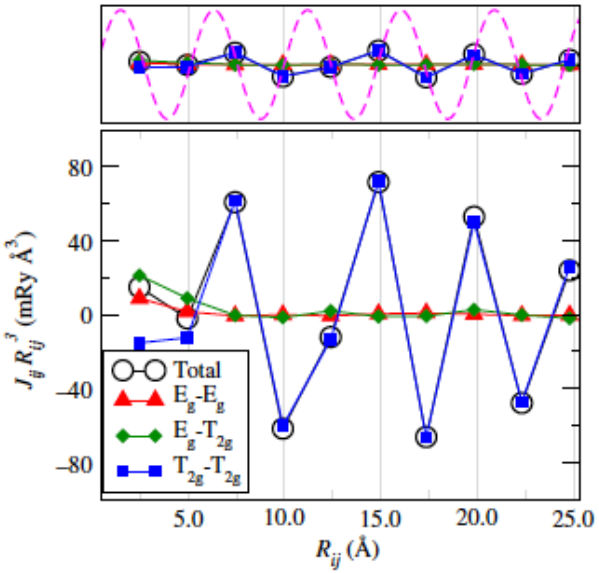

T_{2g}-T_{2g} interactions are long ranged.
Also they are the dominant interactions.

PRL **116**, 217202 (2016)

Analysis of electronic structure

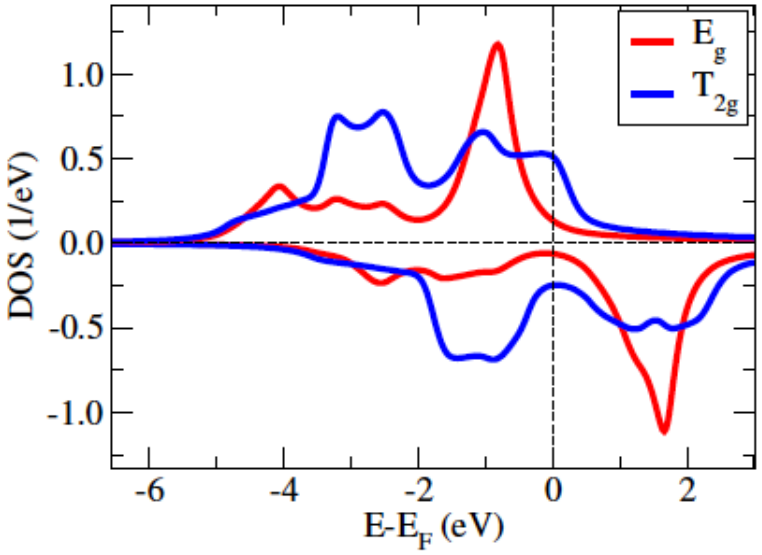

T_{2g} states are dominant at the Fermi level

T_{2g} states contribute to long-range exchange coupling, not E_g.

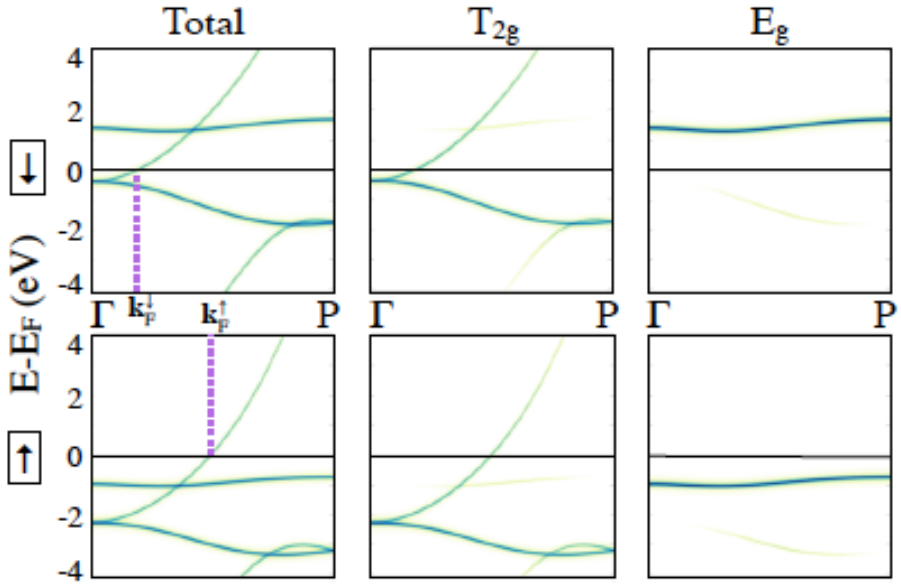

PRL **116**, 217202 (2016)

Finite temperature magnetism (contd.)

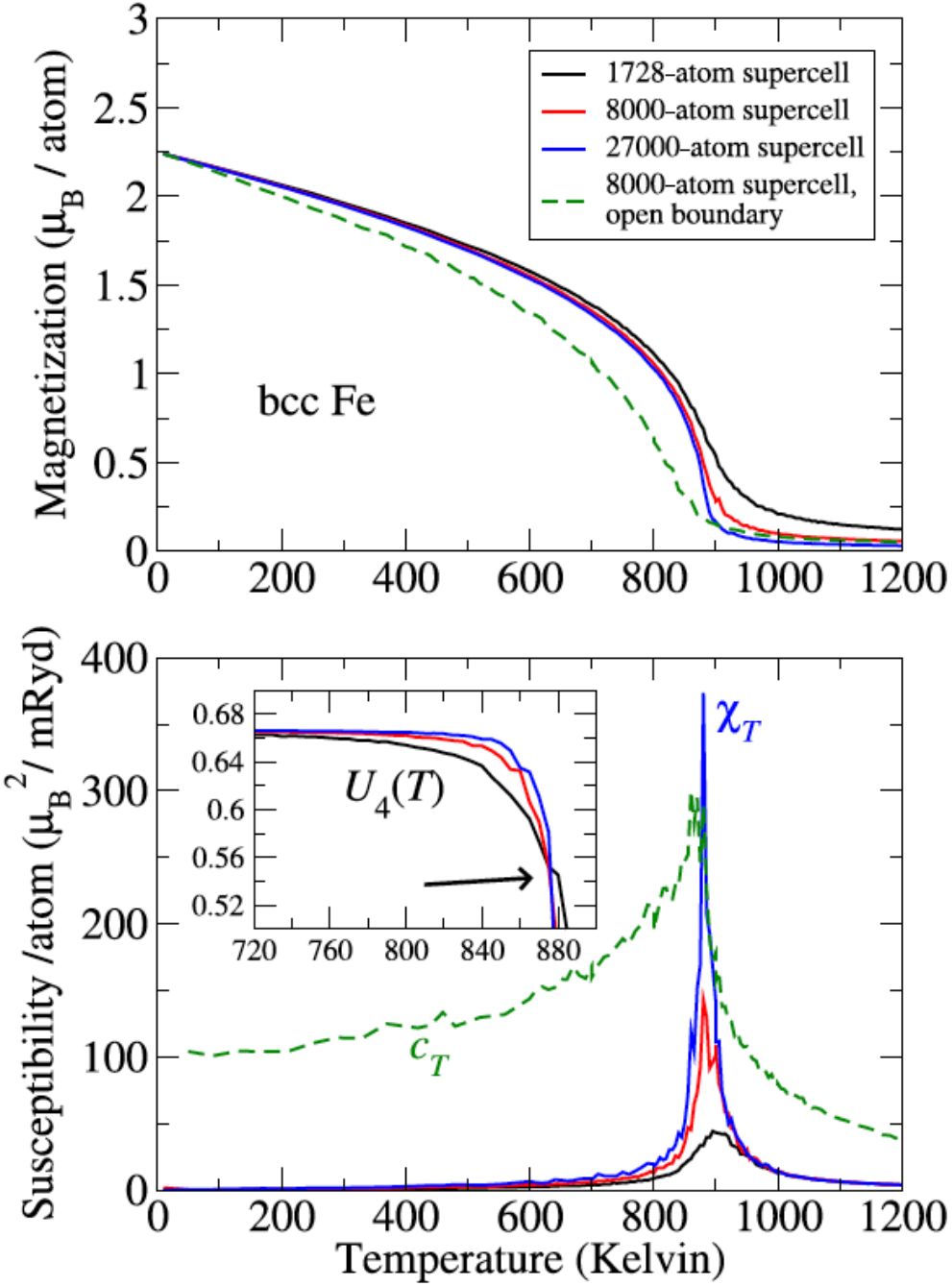

BCC Fe

Experimental T_C: 1043 K

Theoretical T_C: ~900 K

Mavropoulos, IFF Spring School ('14)

Oxides: Monte Carlo simulation

Quadruple perovskite $CaCu_3Fe_2Re_2O_{12}$

Half-metallic, large magnetization, high transition temperature

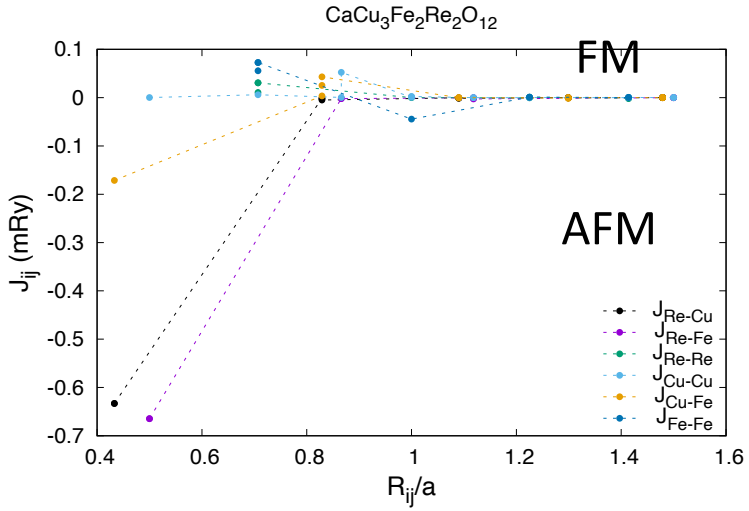

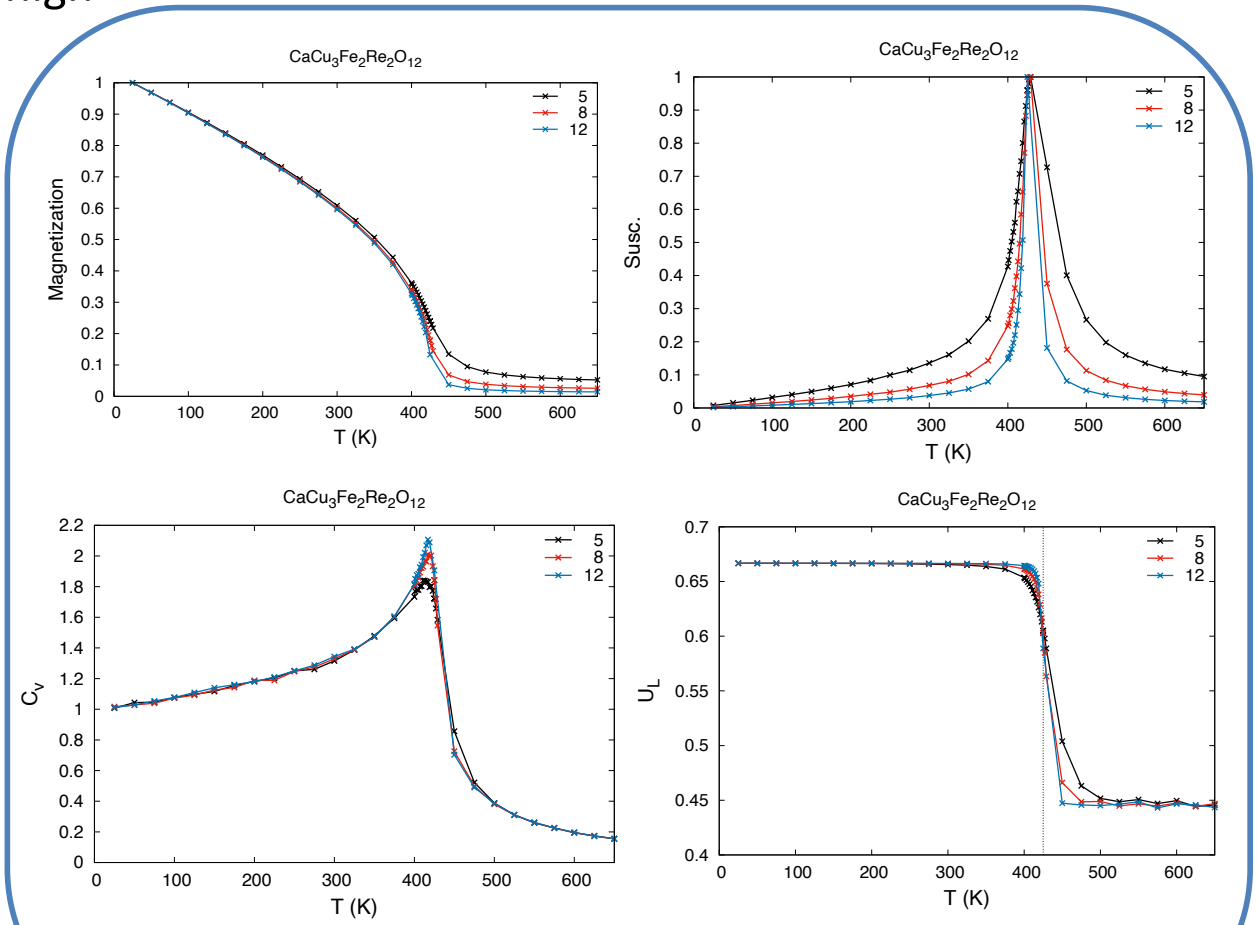

T_c=425K

Wang & Sanyal, unpublished

Atomistic spin dynamics

Landau-Lifshitz-Gilbert equation of motion

$$\frac{d\mathbf{m}_i}{dt} = -\gamma \mathbf{m}_i \times [\mathbf{B}_i + \mathbf{b}_i(t)] - \gamma \frac{\alpha}{m} \mathbf{m}_i \times (\mathbf{m}_i \times [\mathbf{B}_i + \mathbf{b}_i(t)])$$

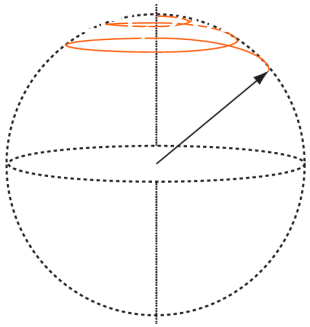

precession

damping

Effective field $\mathbf{B}_i = -\frac{\partial H}{\partial \mathbf{m}_i}$

$\mathbf{b}_i(t)$: Stochastic magnetic field

α : damping parameter

γ : electron gyromagnetic ratio

Exchange (classical Heisenberg)

$$H_{ex} = -\frac{1}{2} \sum_{i \neq j} J_{ij} \mathbf{m}_i \cdot \mathbf{m}_j$$

Dzyaloshinskii-Moriya (spin-orbit coupling)

$$H_{DM} = \sum_{ij} \mathbf{D}_{ij} \cdot (\mathbf{S}_i \times \mathbf{S}_j)$$

Skubic *et al*., J. Phys: Condens. Matt. **20**, 315203 (2008)

Atomistic spin dynamics webpage: http://www.physics.uu.se/cmt/asd

Home grown code: UppASD

Ultrafast magnetization dynamics (ab initio theory + spin dynamics)

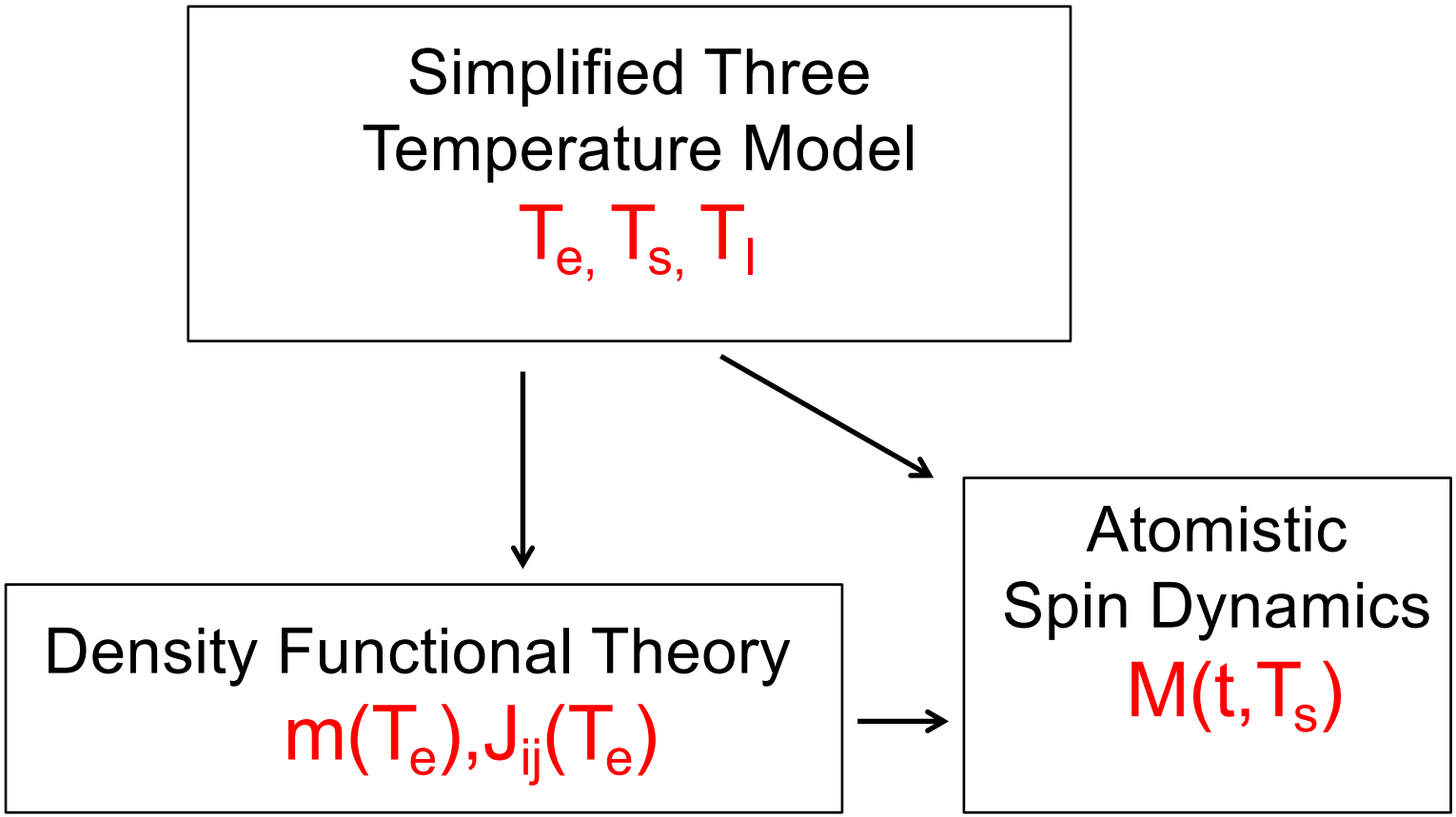

Atomic and macrospin dynamics & time evolution of electron and spin temperatures (bcc Fe)

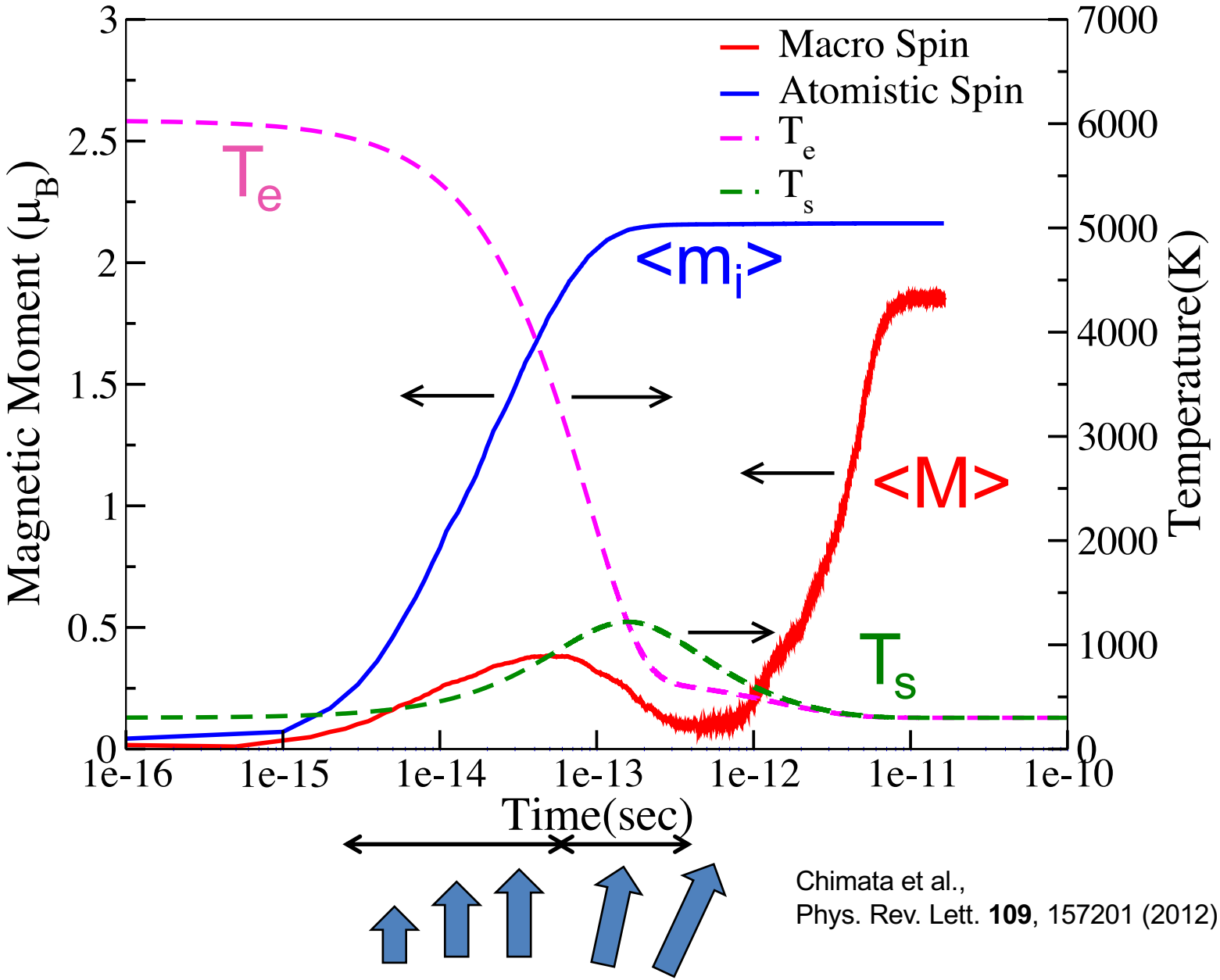

Chimata et al.,
Phys. Rev. Lett. **109**, 157201 (2012)